J. Plasma Fusion Res. SERIES, Vol. 11 (2015)

Correlation of Microstructure Evolution and Hardening in Ion-irradiated Pure Tungsten

Zhexian ZHANG[a,*], Wentuo HAN[b], Akihiko KIMURA[b]

[a] *Graduate School of Energy Science, Kyoto University, Uji, JAPAN*

[b] *Institute of Advanced Energy, Kyoto University, Uji, Japan*

(Received: 17 September 2014 / Accepted: 19 January 2015)

Pure tungsten specimens in cold rolled condition and recrystallized condition were irradiated with 6.4 MeV Fe^{3+} at 300 °C, 700 °C, 1000 °C respectively. The damage profile was calculated by SRIM. The averaged dpa was 2 dpa at 600nm. The irradiation hardness was tested by nano-indentation method with CSM mode and the bulk-equivalent hardness was evaluated by following Nix-Gao model. All the samples showed irradiation hardening irrespective of irradiation temperature and specimen condition. The recrystallized ones showed larger irradiation hardening than the as-received ones. TEM observations revealed that voids were generated at 1000 °C. At the same time, dislocations and loops were found at all the temperatures. No precipitate was found in the irradiated layer. Orowan equation was applied to estimate the strengthening contributed by dislocations, loops and voids. Although it is considered that the contribution of voids is rather small, the estimated hardening based on the TEM observation results are far from the measured one.

Keywords: tungsten, irradiation hardening, recrystallization, void formation

1. Introduction

ITER has selected full-W divertor system in stead of W/CFC[1-3]. The tungsten will endure 0.7 dpa after a neutron loading of 0.15 MWa/m^2 at operation temperatures [4]. During neutron irradiation, radiation damage structures such as dislocation, loops and voids, and precipitates including transmutation helium atoms will be generated and they may cause the deterioration of mechanical properties. These structures will block dislocation motion and cause irradiation hardening. Since irradiation hardening is often accompanied by loss of ductility, understanding hardening mechanism is necessary.

Microstructure evolution induced by neutron irradiation in tungsten and its alloys at different temperatures were summarized by several researchers [5,6]. Loops are generated at low displacement per atom (dpa) and voids were found in many irradiation conditions. As irradiation temperature increases or dpa increases, loops are more likely replaced by voids. In the case of high temperature irradiation over 1000°C, voids were generated and considered to behave as pinning obstacles for dislocations that account for hardening effect [7].

Since neutron irradiation consumes more time and financial cost, ion-irradiation has often been used to obtain high damage level within shorter time and with lower expense [8-11]. The ion-accelerator, DuET, in Kyoto University offers 6.4MeV Fe^{3+} irradiation beam and the irradiation temperatures are controlled by an infrared thermal temperature control system. In this paper, pure tungsten before and after recrystallization condition was irradiated by DuET at 300°C, 700°C and 1000°C. The hardness was measured by continuous stiffness measurement (CSM) by nano-indentation method and microstructures were observed by TEM at 200keV. Irradiation hardening was correlated with microstructure evolution.

2. Experimental procedure

The material used was a commercial pure tungsten (99.95%, Nilaco Corporation) and the texture was shown in Fig. 1 which was investigated by EBSD analysis performed on ZEISS Ultra55 with EBSP detector. A specimen was annealed at 1400 °C for 1 h and called as recrystallized specimen hereafter. All the specimens were polished by #500, #800, #1200, #2400, and #4000 SiC paper, followed by diamond polishing with the diameter of 6μm, 3μm, 1μm and 0.25μm powders. The final electrical polishing was done in 2% NaOH solution under 15 V for 2 min. Vickers hardness measurement was carried out for specimens before

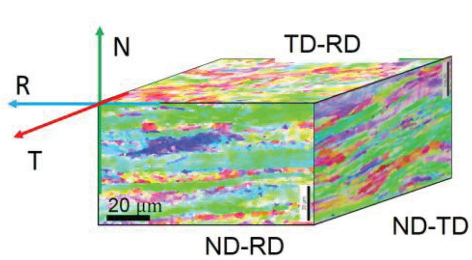

Fig.1 EBSD analysis of as-received tungsten plate. The grains of NR and NT surface are elongated and grains on TR are isotropic.

author's e-mail: zx-zhang@iae.kyoto-u.ac.jp

irradiation using ASAHI HM-103-HH with a load of 0.1 kgf holding for 10s.

The ion-irradiation was carried out on as-received TR surface, NR surface and recrystallized TR surface of tungsten sheets, respectively. The damage profile was calculated by SRIM-2013[12] with different methods by the following equations: (1) full damage cascade, FC, (2) quick calculation of damage, vacancy model, (3) quick calculation of damage, NRT model, QD [13]. In equation (3), T_{dam} means the energy loss to ions and phonons, ED [14]. Here the author uses the average of 2 dpa at 600nm depth from the result of ED method to present for the irradiation displacement damage.

$$dpa = \frac{vacancies + replacement}{atom\ density} \times fluence \quad (1)$$

$$dpa = \frac{vacancies + recoils}{atom\ density} \times fluence \quad (2)$$

$$dpa = \frac{0.8T_{dam}}{2E_d} \times fluence \quad (3)$$

Nano-indentation hardness was measured by CSM method. The indentation depth was 2000 nm and oscillation was selected as 1 nm. Nix-Gao model (Fig.3) was used to calculate the bulk-equivalent hardness [15]. Microstructures were observed by JEOL-2010 TEM at 200keV. The samples were prepared by FIB (JFIB-2100) with Ga^{3+} and then ion-milled with Model 1040 NanoMill with 900eV Ar^{+}.

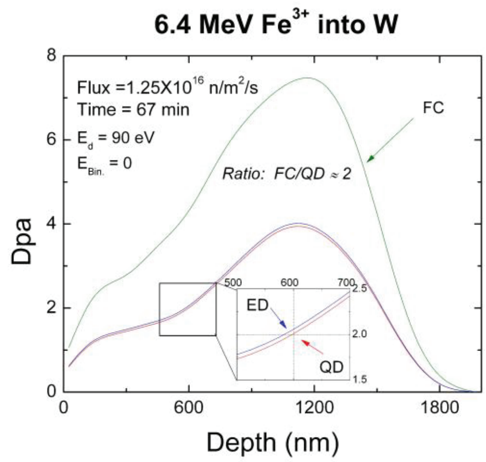

Fig.2 Displacement damage profile calculated by SRIM. Nominal 2 dpa at 600 nm was selected as the damage level.

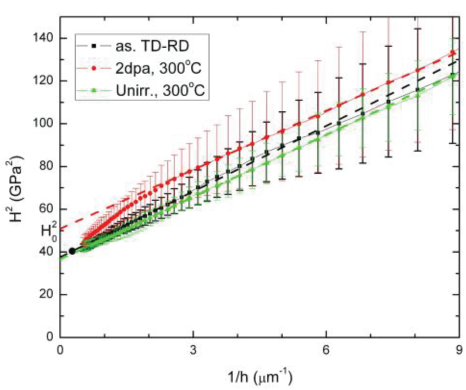

Fig.3 The bulk-equivalent hardness, H0, based on Nix-Gao model. The irradiated curve has a shoulder which is considered as soft substrate effect.[16]

3. Result and discussion

The temperature dependence of irradiation hardening of pure tungsten before and after recrystallization was shown in Fig.4. All of the samples showed hardening at all the temperatures. The recrystallized tungsten showed a higher irradiation hardening than as-received ones. This is reasonable that the recrystallization eliminated most of the grain boundaries which acts as absorption sink site of irradiation induced interstitials and vacancies. As for temperature dependence, as the temperature increases, the hardening increases in the case of before recrystallization, while the recrystallized ones remain stable. Comparing the specimens with different surface direction of as-received, no difference was found between TR and RN, indicating that the grain shape change is not effective to change the amount of hardening.

Nano-hardness test is very sensitive to the surface condition and testing environment. Any disturbance could cause a big error. The total of absolute deviations makes it even more difficult to present the accurate value. In general, however, the trend of the curve is good enough, and the irradiation hardening was calculated by ΔHV=HV(irr.) - HV(unirr.). The error was calculated by $err(\Delta HV) = \sqrt{err(HVirr.)^2 + err(HVunirr.)^2}$.

The microstructures after ion-irradiation are shown in Fig.5, which indicates high number densities and large diameters of voids in the specimen irradiated at 1000 °C. No void was observed in the specimens irradiated at 300 °C and 700 °C. The high temperature may excite the mobility of vacancy clusters in stage IV [17] which

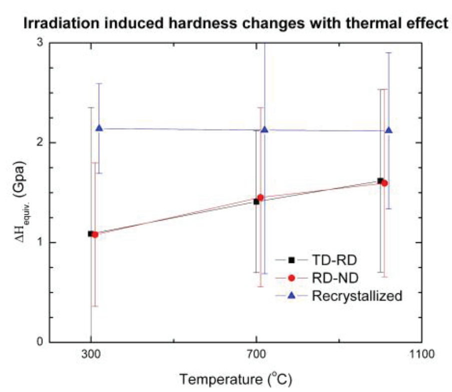

Fig.4 Temperature dependence of irradiation hardening of pure tungsten before and after recrystallization.

corresponds to the dissociation of $V_{n\geq5}$ formed in stage III [18]. At the same time, impurities will suppress the tendency of resolvable voids formation because impurities could serve as individual trapping sites for vacancies[19]. This could be the reason why voids were found in other papers[5-6,8] but not in this experiment.

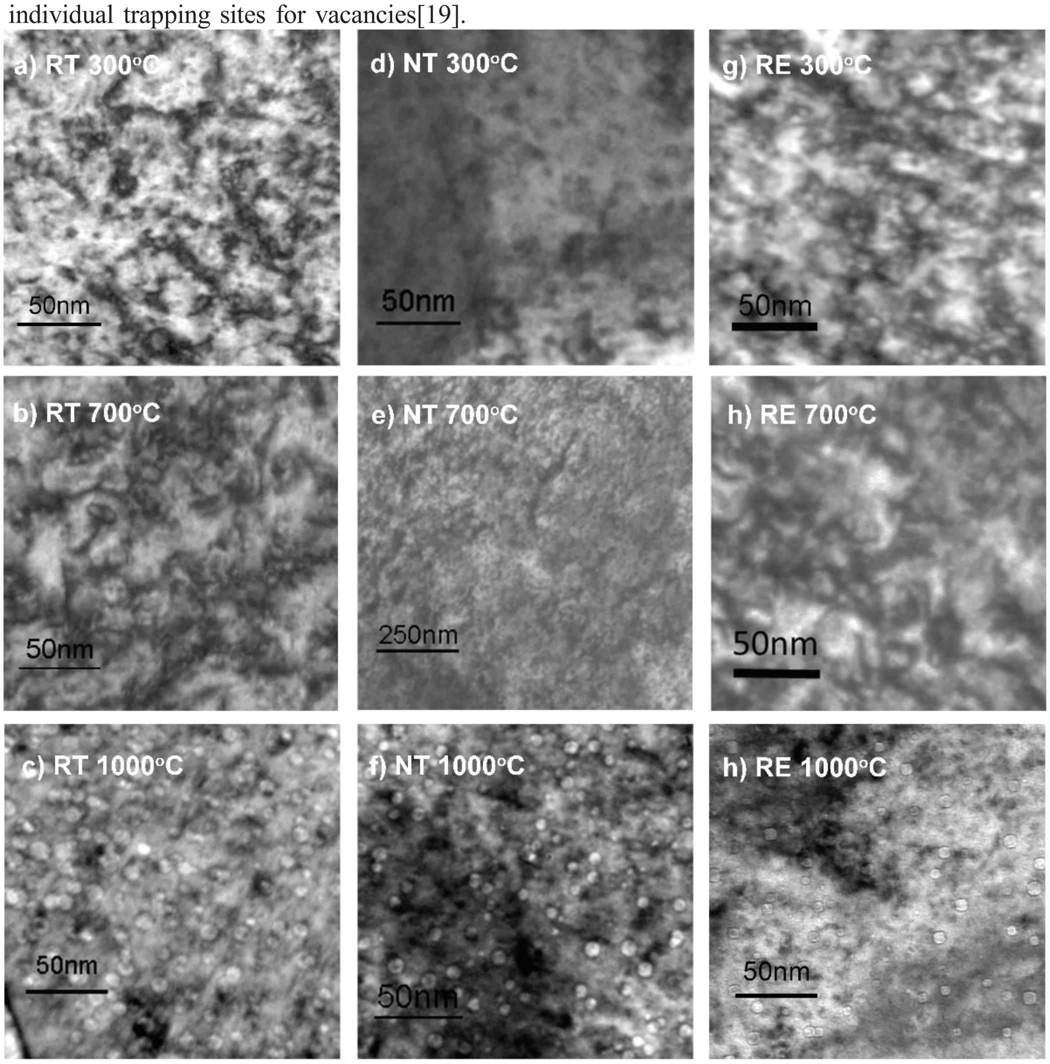

Fig.5 Microstructures observed by TEM. Voids were found in all the specimens irradiated at 1000°C, while in the specimens irradiated at 300°C and 700°C, only the dislocations and loops were formed. The photos, a), b), d), e) g), and h) were observed in just focus condition. c), f), and i) were taken in the under focused condition.

Table.1 Mean diameter and number density of dislocation/loops, voids, and the hardness estimated and measured.

Fe^{3+}into W	dislocation		Loops				Voids $(Nd)^{1/2}$		ΔH(GPa)	
			Number	Size	$(Nd)^{1/2}$	ΔH				
2dpa	$10^{14}/m^2$	ΔH	$10^{22}/m^3$	nm	$X10^6/m$	GPa	$X10^6/m$	ΔH	Estimated	Measured
TR,300°C	4.23	1.27	1.28	4.72	7.77	0.54			1.81	1.09
TR,700°C	5.70	1.47	1.38	5.21	8.48	0.57			2.04	1.41
TR,1000°C	4.64	1.33	1	6.51	8.07	0.55	20.6	1.27	3.15	1.62
Re,300°C	6.40	1.56	1.02	7.99	9.03	0.58			2.14	2.14
Re,700°C	8.36	1.78	8.7	9.5	9.09	0.59			2.37	2.12

Loops and dislocations were found in the 300°C 700°C and 1000°C. Dislocation number density was calculated by line intercept method and computed by $\rho = N/L_r t$. N is the number of intercept points. L_r is the total length of random lines and t is the thickness of TEM foil, which was measured by CBED technique.

For bcc metals, after irradiation, the Burgers vectors of dislocation loops are mainly 1/2<111> and <100>. Assume the density of ½<111> loops was a, and <100> loops was b. Images were taken at different reflection conditions: [200], [110], [211] and the densities in each condition were recorded as A, B, C. According to invisibility criterion g·b=0 (ignoring edge component), we have the visible fraction at each reflection condition:

$$\begin{pmatrix} 1 & 1/3 \\ 1/2 & 2/3 \\ 3/4 & 1 \end{pmatrix} \begin{pmatrix} a \\ b \end{pmatrix} = \begin{pmatrix} A \\ B \\ C \end{pmatrix} \tag{4}$$

Solution of this equation is:

$$\begin{pmatrix} a \\ b \end{pmatrix} = \begin{pmatrix} 4/3 & -2/3 \\ -1 & 2 \end{pmatrix} \begin{pmatrix} A \\ B \end{pmatrix} \tag{5}$$

Or

$$\begin{pmatrix} a \\ b \end{pmatrix} = \begin{pmatrix} 4/3 & -4/9 \\ -1 & 4/3 \end{pmatrix} \begin{pmatrix} A \\ C \end{pmatrix} \tag{6}$$

So that total dislocation/loop density is:

$$a + b = \frac{1}{3}A + \frac{4}{3}B \tag{7}$$

or

$$a + b = \frac{1}{3}A + \frac{8}{9}C \tag{8}$$

Grain boundaries were considered to be able to absorb the defects generated from irradiation, these defects include interstitial atoms and vacancies. Recrystallization will eliminate such grain boundaries. As the migration energy of interstitials is much smaller than that of vacancies, even though there were no voids found in 300°C and 700°C irradiated samples, the accumulated interstitial atoms could form into and be absorbed by loops and line dislocations. Thus, in recrystallized samples, the elimination of grain boundaries will lead to higher number of interstitials comparing to as-received ones, and therefore a higher number density of dislocations as well.

Orowan equation (equation 9) was used to estimate the hardening related to the microstructures observed by TEM. $\Delta\sigma_y$ stands for yield stress increase caused by obstacles. Taylor factor, *M*, is selected as 6. The factor α is 0.2 for all the microstructures. Burgers vector *b* for tungsten is 0.274 nm. The shear modulus μ is 151 GPa.

$$\Delta\sigma_y = M\alpha\mu b\sqrt{Nd} \tag{9}$$

$$\Delta HV(MPa) = 3\Delta\sigma_y(MPa) \tag{10}$$

The relation between Vickers hardness and nano-indentation could be expressed in the following equation based on the relationship between HV and nano-hardness obtained from experiments in our lab:

$$H_0[GPa] = 0.001268 \times H_v[MPa] \tag{10}$$

The estimated values are shown in Table.1. The hardening values caused by loops are almost the same among the specimens irrespective of irradiation temperature and recrystallization treatment. A remarkable difference is observed for the case of irradiation at 1000 °C because of where the contribution of voids to the hardening was taken into account. However, the large difference of the calculated value from the measured one, indicates that the voids are not effective obstructs to dislocation motion. In this case, strengthening factor, α, of voids could be very small.

Impurities may also contribute to the hardening effect, which will act as obstacles to dislocation motion. However we didn't find any visible precipitate by TEM observation. Another possibility is that very fine invisible voids by TEM existed in the specimens irradiated at 300 °C and 700 °C, while some of the dislocations and loops were induced by FIB and involved in the estimation. There may be residual dislocation and loops that shouldn't account for the hardening. Further investigation is necessary for the determination of the hardening factor α in equation (9).

4. Conclusion

Pure tungsten in as-received and recrystallized conditions were irradiated with Fe^{3+} at 300 °C, 700 °C and 1000 °C up to a nominal displacement damage of 2 dpa. The following results were obtained:

1) Irradiation hardening was observed at all the irradiation temperatures, 300°C, 700°C, 1000°C.
2) Dislocation loops were observed at all the temperatures, while cavities were only observed at 1000°C. The hardening appears to be due to the formation of dislocation loops and possibly due to voids as well at 1000°C.
3) Recrystallized W showed a higher irradiation hardening than as-received W.
4) Large voids were found in 1000°C irradiated samples. The density in recrystallized W is about two times higher than as-received W.
5) Orowan analysis showed similar contribution of dislocation loops to hardening, except the cases when large voids were formed. It is considered that large voids are ineffective in irradiation hardening. Fine voids may contribute to the difference. The Orowan analysis needs further investigation focusing on irradiation temperature dependence.

Acknowledgements

The first author is sponsored by China Scholarship Council. Mr. Hayashi and Dr. Kondo are gratefully acknowledged for the technical support in operation of FIB, TEM, Nanomill. Mr. Okinobu Hashitomi is thanked for the ion-irradiation experiments.

References

[1] T. Hirai et al., Fusion Eng. Des. 88 (2013) 1798-1801.
[2] R.A. Pitts et al., J. Nucl. Mater. 438 (2013) S48-S56.
[3] F. Escoubiac et al., 24th IAEA Fusion Energy Conference, San Diego, 2012, ITR/P5-08.
[4] H. Bolt et al, J. Nucl. Mater. 307-311(2002) 43-52.
[5] A. Hasegawa et al., Mater. Trans., Vol. 54, No. 4 (2013) 466-471.
[6] A. Hasegawa et al. Fusion Eng. Des. 89 (2014) 1568-1572.
[7] R.C. Rau et al., J. Nucl. Mater. 33 (1969) 324-327.
[8] Y. Himei et al., Materials transactions, vol. 54, No. 4 (2013) 446-450.
[9] D.E.J. Armstrong et al., J. Nucl. Mater. 432 (2013) 428-436.
[10] H. Wang et al., J. Nucl. Mater. 442 (2013) 189-194.
[11] X. Yi et al., Philosophical Magazine 93-14 (2013) 1715-1738.
[12] http://www.srim.org/
[13] M.J. Norgett et al., Nucl. Eng. Des. 33:1 (1975) 50-54.
[14] R.E. Stoller et al., Nucl. Instr. Meth. Phys. Res. B 310 (2013) 75-80.
[15] W.D. Nix and H.J. Gao, J. Mech. Phys. Solids, Vol.46, No.3 (1998) 411-425.
[16] R. Kasada et al., Fusion Eng. Des. Vol.86 (2011) 2658-2661.
[17] L.K. Keys et al., Vol. 176, No.3 (1968) 851-856.
[18] C.C Fu et al., Nature Mater. 4, (2005) 68-74.
[19] R.C. Rau et al., J. Nucl. Mater. 33 (1969) 324-327.